Carbon−Proton Chemical Shift Correlation in Solid-State NMR by Through-Bond Multiple-Quantum Spectroscopy

Anne Lesage, Dimitris Sakellariou, Stefan Steuernagel,† and Lyndon Emsley*

Contribution from the Laboratoire de Stéréochimie et des Interactions Moléculaires, UMR CNRS/ENS, Ecole Normale Supérieure de Lyon, 69364 Lyon, France, and Bruker Analytik GmbH, Silberstreifen, 76287 Rheinstetten, Germany

Received August 24, 1998. Revised Manuscript Received October 21, 1998

Abstract: A new two-dimensional NMR carbon−proton chemical shift correlation experiment, the MAS-J-HMQC experiment, is proposed for natural abundance rotating solids. The magnetization transfer used to obtain the correlations is based on scalar heteronuclear *J* couplings. The 2D map provides through-bond chemical shift correlations between directly bonded proton−carbon pairs in a way similar to that in corresponding high-resolution liquid-state experiments. The transfer through *J* coupling is shown to be efficient and more selective than those based on heteronuclear dipolar couplings. The experiment, which works at high MAS spinning frequencies, yields the unambiguous assignment of the proton resonances. The experiment is demonstrated on several organic compounds.

1. Introduction

Unlike rare nuclei such as carbon-13 or nitrogen-15, which give high-resolution solid-state NMR spectra under magic angle spinning (MAS) conditions, the proton spectra of powdered organic molecules yield broad resonances due to the strong homonuclear proton−proton dipolar couplings. However, the characterization of proton spectra in solid-state NMR is of considerable interest, since proton chemical shifts provide a powerful source of characterization for analytical applications as well as yielding additional structural information for more detailed studies. Proton line widths can be partially reduced by using CRAMPS (combined rotation and multiple pulse spectroscopy) techniques,[1−3] which average out the homonuclear dipolar couplings. However, the improvement in resolution often remains insufficient to characterize the proton spectra, even in relatively simple molecular systems. One way to unravel the overlapping one-dimensional proton spectra is to combine homonuclear decoupling techniques with two-dimensional heteronuclear correlation (HETCOR) experiments, which correlate the protons with a rare nucleus such as carbon-13.[4−6] These correlation techniques have been numerously applied to the structural study of organic molecules or biological systems in the solid state.[7−11] It has recently been demonstrated that, by using the frequency-switched Lee−Goldburg (FSLG) technique as the homonuclear decoupling scheme, the HETCOR experiment is practicable at moderately fast MAS frequencies,[12] making the experiment useful for relatively complex molecular systems. Additionally, proton spectral resolution may be improved at the higher B_o field strengths that are currently available. Thus, the proton is becoming an increasingly attractive probe nucleus in the development of structural studies by solid-state NMR.

All of the carbon−proton correlation experiments which have been reported so far are based on a dipolar coupling driven magnetization transfer. Various schemes for polarization transfer have been proposed, ranging from simple Hartman−Hahn cross-polarization to WIM multiple-pulse sequences,[4,5,13] and tested with regard to their sensitivity and distance selectivity. Since all of these experiments act through space, one of the main problems is to ensure a sufficient selectivity in the magnetization transfer for the spectrum to be usefully interpreted, i.e., to transfer magnetization only to directly bonded carbon nuclei and not to carbon nuclei that are further away. While correlation peaks between nonbonded pairs can provide valuable information on the conformation of the molecule, they dramatically complicate the initial analysis of the 2D spectrum.

We have recently shown[14] that heteronuclear scalar couplings can be resolved in powder samples under MAS. In this paper, we report a new two-dimensional proton−carbon correlation experiment which relies on a polarization transfer using heteronuclear J_{CH} couplings and which we call MAS-J-HMQC. In analogy to liquid-state HMQC experiments, the sequence uses heteronuclear multiple quantum coherences to provide isotropic chemical-shift correlation between pairs of directly bonded

† Bruker Analytik GmbH.

* To whom correspondence should be addressed. E-mail: Lyndon.Emsley@ens-lyon.fr.

(1) Taylor, R. E.; Pembleton, R. G.; Ryan, L. M.; Gerstein, B. C. *J. Chem. Phys.* **1979**, *71*, 4541−4545.
(2) Burum, D. P.; Rhim, W. K. *J. Chem. Phys.* **1979**, *71*, 944.
(3) Virlet, J. *The Encyclopedia of NMR*; J. Wiley & Sons: London, 1997.
(4) Caravatti, P.; Bodenhausen, G.; Ernst, R. R. *Chem. Phys. Lett.* **1982**, *89*, 363−367.
(5) Caravatti, P.; Braunschweiler, L.; Ernst, R. R. *Chem. Phys. Lett.* **1983**, *100*, 305−310.
(6) Burum, D. P. *The Encyclopedia of NMR*; J. Wiley & Sons: London, 1997.
(7) Burum, D. P.; Bielecki, A. *J. Magn. Reson.* **1991**, *94*, 645−652.
(8) Bronnimann, C. E.; Ridenour, C. F.; Kinney, D. R.; Maciel, G. E. *J. Magn. Reson.* **1992**, *97*, 522−534.
(9) Lee, C. W. B.; Griffin, R. G. *Biophys. J.* **1989**, *55*, 355−358.
(10) Santos, R. A.; Wind, R. A.; Bronnimann, C. E. *J. Magn. Reson. B* **1994**, *105*, 183−187.
(11) Gu, Z.; Ridenour, C. F.; Bronnimann, C. E.; Iwashita, T.; McDermott, A. *J. Am. Chem. Soc.* **1996**, *118*, 822−829.
(12) vanRossum, E. J.; Förster, H.; deGroot, H. J. M. *J. Magn. Reson.* **1997**, *124*, 516−519.
(13) Roberts, J. E.; Vega, S.; Griffin, R. G. *J. Am. Chem. Soc.* **1984**, *106*, 2506−2512.
(14) Lesage, A.; Steuernagel, S.; Emsley, L. *J. Am. Chem. Soc.* **1998**, *120*, 7095−7100.

10.1021/ja983048+ CCC: $15.00
Published on Web 12/04/1998

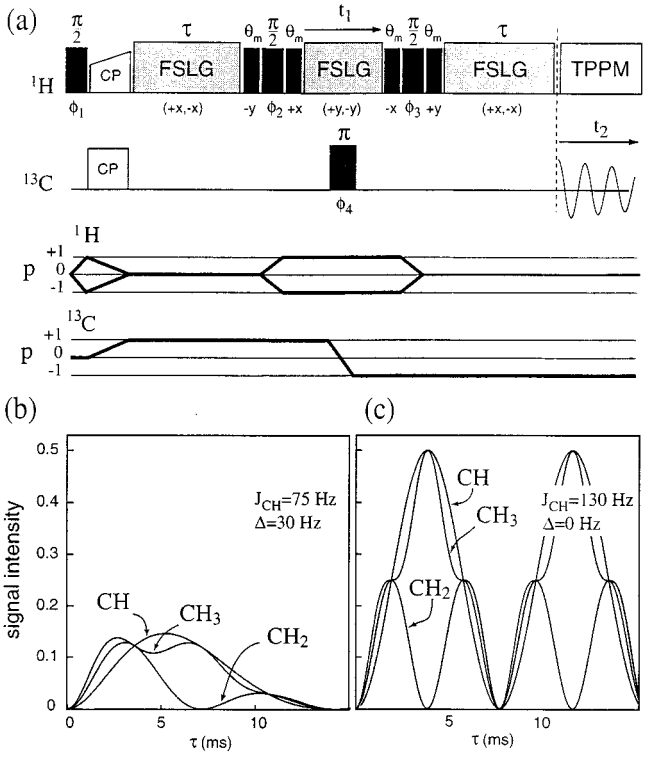

Figure 1. (a) Pulse sequence and coherence transfer pathways[30] for the MAS-J-HMQC experiment. θ_m is a 54.7° pulse. The phases ϕ_1, ϕ_2, and ϕ_3 are cycled to select changes of $p = \pm 1$ (two-step phase cycles for each of the three pulses). Additional phase cycling on the 180° carbon pulse can be added to suppress artifacts. (The pulse program is available from our website[24] or by request to the authors.) The theoretical evolution of the carbon signal intensity as a function of τ is shown in b and c. For each CH_n group ($n = 1-3$), the curves were obtained using the following expressions: $I_{CH_3} = {}^1/_2 I^0_{CH_3}(3c^2s + s^2c) \times \exp(-2\tau/T_2^{CH_3})$; $I_{CH_2} = {}^1/_2 I^0_{CH_2}(2sc) \exp(-2\tau/T_2^{CH_2})$; $I_{CH} = {}^1/_2 I^0_{CH}(c) \times \exp(-2\tau/T_2^{CH})$, with $c = \cos^2(\pi J_{CH}\tau)$, and $s = \sin^2(\pi J_{CH}\tau)$, and where I^0 is the signal intensity after cross polarization and T_2 the transverse relaxation (dephasing) time during the 2τ period ($T_2 = 1/\pi\Delta$). Δ is the full line width at half-height of one component in a *J*-coupled multiplet. The expressions were calculated using product operator algebra[31] and a liquid-like *J* coupling Hamiltonian. Note that the signal intensity of a CH_3 carbon contains two distinct contributions having different functional dependencies: one from a pure double-quantum coherence between the carbon and one proton and one contribution from four-spin coherence. The calculations are shown for two different values of Δ and J_{CH}, as indicated, corresponding to the solid-state case and the equivalent "ideal liquid state" case; 130 Hz is a typical value for a one-bond J_{CH} coupling for an aliphatic carbon, and the value of 75 Hz corresponds to a scaling factor of $1/\sqrt{3}$ due to the FSLG decoupling. These couplings are usually much larger than the two- or three-bond couplings, which can be neglected to first order (see text).

nuclei. We show that the experiment is sensitive and that scalar couplings provide a much more selective means of correlation than dipolar couplings. The experiment can be applied using high spinning frequencies and, provided that the carbon spectrum is assigned, leads to the unambiguous identification of proton chemical shifts in solids.

2. Pulse Scheme

The pulse sequence for the MAS-J-HMQC experiment is shown in Figure 1a. After cross-polarization from ^{1}H (*I* spins), the magnetization of carbons (*S* spins) evolves during the delay τ under only an isotropic scaled heteronuclear J_{CH} coupling Hamiltonian. During this period the proton−proton dipolar couplings are removed by using FSLG,[15,16] whereas the remaining inhomogeneous interactions, i.e., the chemical shift and the heteronuclear dipolar couplings, are averaged by rapid magic angle spinning to their isotropic components, leaving only the isotropic chemical shift and the heteronuclear scalar coupling. For a pair of covalently bonded ^{1}H−^{13}C spins, the carbon magnetization evolves from in-phase (S_x) into antiphase ($2I_zS_y$) coherence with respect to the attached proton. A 90° pulse applied on protons transforms the antiphase carbon coherence into a double-quantum heteronuclear coherence which evolves during t_1 only under the effect of the proton chemical shift. Carbon chemical shift evolution during t_1 (and during the periods τ) is refocused by the 180° pulse applied in the middle of the pulse sequence. Heteronuclear multiple-quantum (MQ) coherences are insensitive to heteronuclear couplings between the two spins involved in the coherence; proton−proton dipolar couplings are removed during t_1 by the FSLG decoupling and the residual heteronuclear dipolar couplings to other spins by MAS and the 180° pulse. At the end of the t_1 evolution period, the MQ coherence is converted back into an antiphase carbon coherence by the second 90° proton pulse. During the second τ period this coherence evolves to become an in-phase observable carbon coherence.

Under FSLG decoupling, the effective field is aligned with the magic angle, i.e., it lies along an axes inclined at 54.7° with respect to the B_o field. The first 54.7° "magic angle pulse" applied on protons at the end of the first τ period compensates for the tilted precession around this axis by rotating the proton longitudinal magnetization into the *z* axis of the rotating frame. In the same way, the second and third magic angle pulses applied on both sides of the t_1 evolution period bring the proton transverse magnetization perpendicular to the effective field and back to the (*x*,*y*) plane, respectively. The fourth magic angle pulse rotates the proton longitudinal magnetization from the *z* axis to the tilted axis so that it is aligned with the effective field during the second τ delay. The magic angle pulses associated with the τ periods serve to increase the sensitivity of the experiment, while those associated with t_1 serve also to minimize axial peaks and quadrature images.

During the acquisition period, TPPM[17] heteronuclear decoupling is applied. A two-dimensional Fourier transform yields pure in-phase chemical shift correlations between pairs of bonded protons (in ω_1) and carbons (in ω_2). Due to the FSLG sequence, the heteronuclear couplings as well as the proton chemical shift in ω_1 are scaled by a factor $1/\sqrt{3}$. Note that for a CH_2 or CH_3 group, higher orders of coherences are created at the end of the τ evolution period, i.e., triple or quadruple heteronuclear MQ coherences. However, the phase cycle on ϕ_2 and ϕ_3 (Figure 1) selects only the double-quantum heteronuclear coherences. Also note that the MAS-J-HMQC experiment has many aspects in common with the well-known HMQC[18] liquid-state NMR experiment.

Figure 1b,c shows the theoretical evolution curves of the intensity of the observable magnetization as a function of the delay τ. These curves were calculated for all types of carbon multiplicity in the "solid-state" case (Figure 1b) and compared for reference to the "ideal liquid-state" case (Figure 1c). In solid

(15) Bielecki, A.; Kolbert, A. C.; Levitt, M. H. *Chem. Phys. Lett.* **1989**, *155*, 341.
(16) Levitt, M. H.; Kolbert, A. C.; Bielecki, A.; Ruben, D. J. *Solid State NMR* **1993**, *2*, 151−163.
(17) Bennett, A. E.; Rienstra, C. M.; Auger, M.; Lakshmi, K. V.; Griffin, R. G. *J. Chem. Phys.* **1995**, *103*, 6951.
(18) Bax, A.; Griffey, R. H.; Hawkins, B. L. *J. Magn. Reson.* **1983**, *55*, 301−315.

samples, the effective scalar coupling is reduced by the scaling factor of the FSLG decoupling sequence (a J_{CH} coupling of 130 Hz, which is a typical value for a sp^3 carbon in hydrocarbons,[19] will give an effective scaled coupling of 75 Hz) and a line broadening of several tens of hertz has to be considered which strongly attenuates the signal intensity by transverse relaxation. However, if the FSLG sequence applied during the 2τ period is efficient enough to yield line widths comparable to the size of the scaled heteronuclear scalar coupling, then a significant signal should be observed, rendering the experiment practicable. The optimal delay to excite double-quantum heteronuclear coherences, independent of the number of attached protons, is about 2 ms.

3. Experimental Section

The (natural abundance) samples of camphor, L-tyrosine hydrochloride, and cholesteryl acetate were purchased from Sigma and used without further recrystallization. The tripeptide Boc-Ala-Ala-Pro-O-Bzl (where Boc stands for *tert*-butoxycarbonyl and Bzl for benzyl) was synthesized in our laboratory and crystallized from diisopropyl oxide.[20] Approximately 20 mg of each sample was used. The experiments were performed on a Bruker DSX 500 spectrometer (proton frequency 500 MHz) using a 4-mm triple-resonance MAS probe. The sample volume was restricted to about 25 μL in the center of the rotor to increase the radio frequency field homogeneity. With our probe, we found that this was necessary to resolve, under FSLG decoupling, the multiplet fine structure due to scalar J_{CH} couplings in real samples such as L-alanine.[14] The proton radiofrequency (rf) field strength was set to 100 kHz during both the τ delays (FSLG decoupling) and during acquisition (TPPM decoupling). The FSLG sequence consists of two off-resonance pulses with opposite phases (i.e., $+x,-x$ or $+y,-y$) (see Figure 1a) and opposite offsets so that the effective field is always aligned along the magic angle axis. As pointed out previously,[21] we found that the best performance of the FSLG sequence was achieved when we used a mean frequency offset of about 5 kHz from the center of the proton resonance line, i.e., best results were obtained using "asymmetric" offsets. These offsets for FSLG decoupling were carefully adjusted experimentally on a natural abundance sample of L-alanine, for which the multiplet fine structure due to scalar J_{CH} couplings can be resolved. The overall duration of each of the two off-resonance pulses was 8.2 μs ($\omega_1 = 100$ kHz yields a 360° pulse around the 122 kHz total effective field of 8.2 μs). For technical reasons specific to our spectrometer, each pulse was divided into two successive pulses: a 1.25 μs pulse during which the frequency was changed and a pulse of 6.95 μs with the correct phase. This programming was necessary so that the phase and frequency changes occur simultaneously in reality. For the cross-polarization step, the radio frequency field was set to 80 kHz for carbon, while a ramped rf field was applied on protons[22,23] and matched to obtain optimal signal. A 32-step phase cycle was used to select the coherence transfer pathway shown in Figure 1 (pulse program and phase cycle available on our web site[24] or by request to the authors). The τ delay was synchronized to be an integral number of rotor periods. Quadrature detection in ω_1 was achieved using the States-TPPI method.[25] For the dipolar HETCOR of Figure 5b, we used the experiment described by van Rossum et al.[12] In the proton dimensions, reference frequencies were set by analogy with liquid-state spectra (details below).

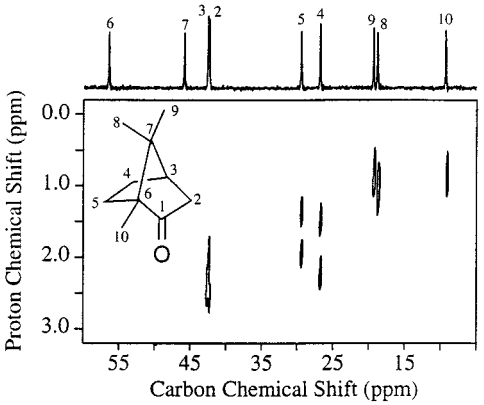

Figure 2. Two-dimensional MAS-J-HMQC spectrum of a powder sample of natural abundance camphor. A total of 256 t_1 increments with eight scans each were collected. The spinning frequency was 6 kHz and τ was set to 2 ms. The 1D CP-MAS ^{13}C spectrum is shown above the 2D spectrum. See Table 1 for details on the proton reference frequency and chemical shifts measured using this spectrum.

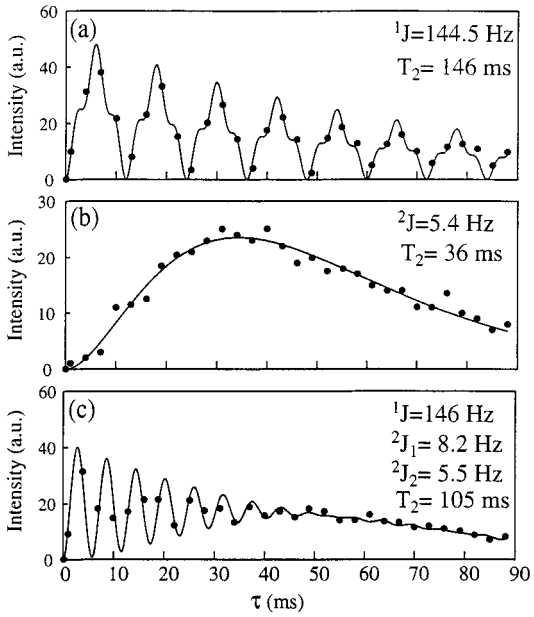

Figure 3. Evolution of the signal intensity in one-dimensional MAS-J-HMQC experiments ($t_1 = 0$) as a function of the τ delay for peaks number 10 (a), 7 (b), and 5 (c) of camphor corresponding respectively to a methyl carbon, a quaternary carbon, and a methylene carbon (spinning frequency 6 kHz). The points are the measured values whereas the solid curves correspond to fittings from analytical expressions (calculated using product operator algebra[31] and a liquid-like J coupling Hamiltonian). The adjustable parameters were the overall intensity, the J_{CH} couplings, and the transverse relaxation time. The simulations were done by considering three equivalent J_{CH} couplings for peak 10 (a), one J_{CH} coupling for peak 7 (b), and two equivalent (one-bond) and two different (two-bond) J_{CH} couplings for peak 5 (c).

4. Discussion

Figure 2 shows the MAS-J-HMQC spectrum recorded on camphor, a plastic crystal having exceptionally narrow line widths. The assignment of the one-dimensional carbon spectrum has been previously reported.[26] As expected, the quaternary carbons (peaks 6 and 7) give no correlation peaks in the 2D map, as they are not directly bonded to any protons, whereas all the protonated carbons are correlated with their attached

(19) Kalinowski, H.-O.; Berger, S.; Braun, S. *Carbon-13 NMR Spectroscopy*; John Wiley & Sons: Chichester, U.K., 1988.
(20) Guy, L.; Vidal, J.; Collet, A.; Amour, A.; Reboud-Ravaux, M. *J. Med. Chem.* **1998**, submitted.
(21) Bielecki, A.; Kolbert, A. C.; deGroot, H. J. M.; Griffin, R. G.; Levitt, M. H. *Adv. Magn. Reson.* **1989**, *14*, 111.
(22) Metz, G.; Wu, X.; Smith, S. O. *J. Magn. Reson. A* **1994**, *110*, 219−227.
(23) Hediger, S.; Meier, B. H.; Kurur, N. D.; Bodenhausen, G.; Ernst, R. R. *Chem. Phys. Lett.* **1994**, *223*, 283−288.
(24) http://www.ens-lyon.fr/STIM/NMR.
(25) Marion, D.; Ikura, M.; Tschudin, R.; Bax, A. *J. Magn. Reson.* **1989**, *85*, 393−399.
(26) Benn, R.; Grondey, H.; Brevard, C.; Pagelot, A. *J. Chem. Soc. Chem. Commun.* **1988**, 102−103.

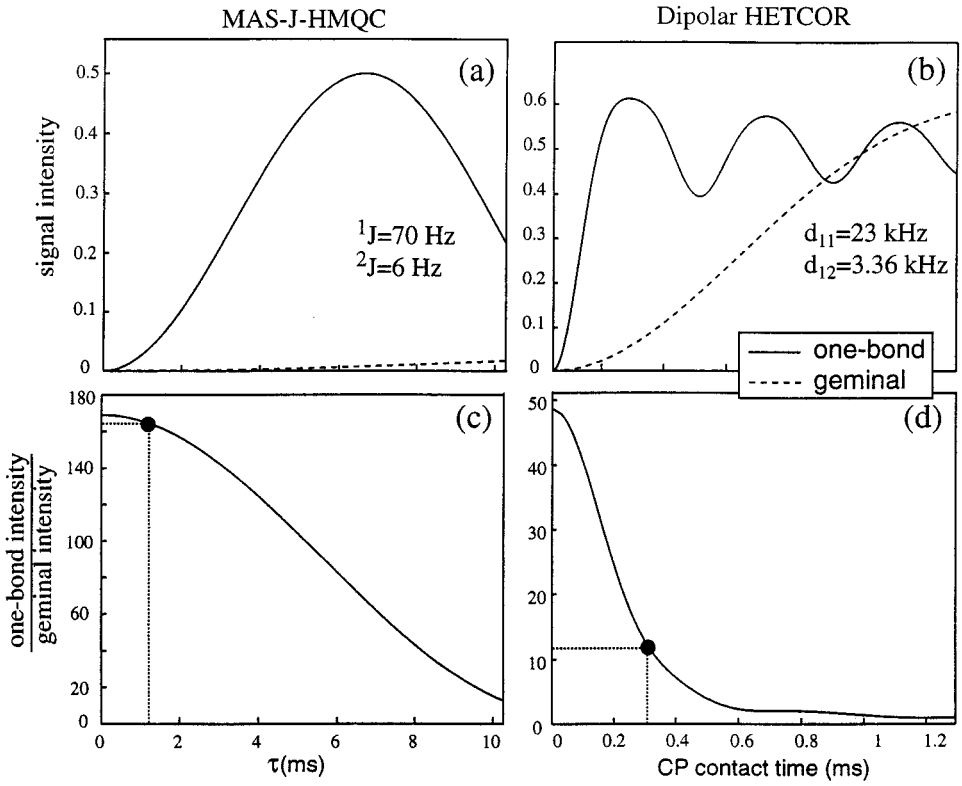

Figure 4. Simulated coherence transfer efficiency as a function of τ in the MAS-J-HMQC experiment (a) and in the dipolar HETCOR experiment (b). In a, the curves were calculated according to the equations given in the caption of Figure 1 for a CH group. The solid line corresponds to transfer through a one-bond J_{CH} coupling (70 Hz), while the dashed line corresponds to the transfer through a two-bond $^2J_{CH}$ coupling (6 Hz). For the dipolar HETCOR experiment (b), a cross-polarization scheme was considered for the polarization transfer. The following expression was used for the calculations[32] $\langle S_x \rangle(t) = [1 - g(t)]/2$, where $(g)t = {}^1/_2 \int_\theta \cos[b(\theta)t] \sin(\theta)\, d\theta$, where $b(\theta)$ is the orientation-dependent dipolar coupling. The calculations were performed for the case of a directly bonded carbon−proton pair, using an internuclear distance of 1.1 Å corresponding to a dipolar coupling of 23 kHz (solid line), and in the case of two geminal nuclei, using a distance of 2.1 Å for a dipolar coupling of 3.3 kHz (dashed line). Relaxation was not taken into account. In c and d, the ratio of the transfer efficiencies between directly bonded and geminal nuclei is represented for the two types of heteronuclear correlation experiments. The MAS-J-HMQC experiment has a better selectivity than the dipolar HETCOR with respect to transfer from closest neighbors. For mixing times of 1.3 ms and 300 μs for the MAS-J-HMQC experiment and the dipolar HETCOR experiment, respectively, the selectivity of transfer is predicted to be 16 times greater in the MAS-J-HMQC than in the dipolar HETCOR.

protons. Note that, for each CH_2 group (peaks 2, 4, and 5), there are two distinct correlation peaks corresponding to the two different chemical shifts of the two (diastereotopic) protons. The proton chemical shifts for camphor can be measured quite straightforwardly and without ambiguity using this MAS-J-HMQC spectrum, and they are listed in Table 1. Note that, while plastic crystals are often considered as trivial examples, it is not possible to obtain this kind of correlation using dipolar methods in plastic crystals since all the intramolecular dipolar couplings are averaged to zero by local molecular motion.

4.1. Long-Range Couplings. The two-dimensional spectrum of Figure 2 was recorded with a short value of τ (2 ms), so that the contribution of two- and three-bond J_{CH} couplings remains negligible. However long-range scalar couplings, which are also active during the evolution periods, can lead to the excitation of heteronuclear double-quantum coherences for longer values of τ. This is illustrated in Figure 3, showing the experimental and simulated evolution of signal intensity as a function of the τ delay for three different carbons: carbon 10 (methyl carbon), carbon 7 (quaternary carbon), and carbon 5 (methylene carbon). For the quaternary carbon (Figure 3b), we observe a significant signal whose evolution can be fitted with a small value of the $^2J_{CH}$ coupling, 5.4 Hz, which is in agreement with the order of magnitude expected for two-bond J_{CH} couplings.[19] The methyl group (Figure 3a) is "isolated" from other protons as can be seen from the molecular structure of camphor, and indeed, its signal evolution as a function of τ can be fitted without taking into account any long-range couplings. Once again the fitted value (144.5 Hz) corresponds well to what can be expected for a one-bond J_{CH} coupling in an organic compound. To fit correctly the experimental data of the methylene carbon 5 (Figure 3c), we accounted for both two equivalent one-bond $^1J_{CH}$ couplings and two different two-bond $^2J_{CH}$ couplings, which would correspond to the couplings with protons 4 (fitted values $^1J = 146$ Hz, $^2J_1 = 8.2$ Hz, and $^2J_2 = 5.5$ Hz). The values for the one-bond J_{CH} couplings found by these fitting procedures are in agreement with the experimental couplings that can be measured in the one-dimensional carbon spectrum acquired under FSLG decoupling (129 and 139 Hz for carbons 10 and 7, respectively, data not shown). Thus, this study on the model sample of camphor confirms that the experiment does yield scalar coupling driven magnetization transfer and shows that two-bond J_{CH} couplings, despite the fact that they are quite small, can also lead to the creation of multiple-quantum heteronuclear coherences. In summary, short values of τ should be used to ensure only one-bond chemical shift correlations.

4.2. Selectivity. The selectivity in terms of one-bond vs many bond transfer of the MAS-J-HMQC experiment can be compared in a semiquantitative manner to that of a dipolar-based HETCOR experiment. This is illustrated in Figure 4 showing the efficiencies of one-bond and geminal transfers in the MAS-J-HMQC experiment (a) and in the dipolar HETCOR experiment (b). In the MAS-J-HMQC experiment, the transfer is oscillatory because the J_{CH} couplings are orientation-independent

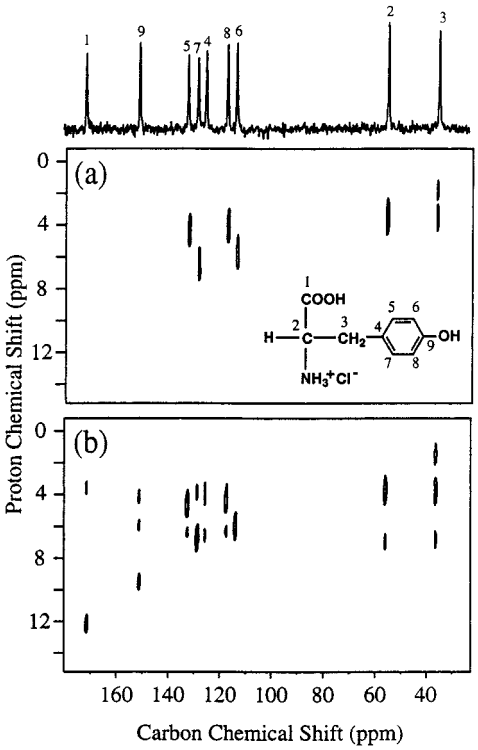

Figure 5. Two-dimensional MAS-J-HMQC spectrum (a) and dipolar HETCOR spectrum (b) of a natural abundance sample of L-tyrosine hydrochloride. The spinning frequency was 15 kHz. τ was set to 1.3 ms for the MAS-J-HMQC experiment, and the contact time for CP in the dipolar HETCOR was 300 μs. A total of 256 t_1 increments with 96 scans each were collected for both experiments.

Table 1. Proton Chemical Shifts for Camphor Measured from a 2D MAS-J-HMQC Spectrum

nuclei	δ (ppm)[a,b]	nuclei	δ (ppm)[a,b]
H_2	2.57, 1.95	H_8	1.07
H_3	2.34	H_9	0.84
H_4	2.21, 1.47	H_{10}	0.88
H_5	1.95, 1.35		

[a] Frequencies in the proton dimension are given with respect to proton H_{10}, which was set to 0.88 ppm with respect to TMS by analogy with a liquid-state spectrum recorded in $CDCl_3$ at 20 °C. [b] Errors on the reported chemical shifts are estimated to be around ±0.05 ppm.

and all the crystallites behave identically. On the other hand, in a cross-polarization experiment, it is well-known that, for an isolated two spin system, the transfer has a damped oscillatory behavior due to integration over the whole powder. As a result, the selectivity of the heteronuclear coherence transfer process is much weaker for the dipolar case as illustrated in Figure 4c,d which compares the ratio of the direct and geminal transfers for the two types of experiments. We see clearly that, in the MAS-J-HMQC experiment, the contribution to the signal intensity of two-bond J_{CH} couplings is proportionally much less than the contribution of geminal dipolar couplings in a dipolar HETCOR experiment. In addition to the difference in dynamics, the difference in selectivity is also related, to a lesser extent, to the fact that the ratio of direct and geminal couplings is more favorable for scalar interactions. Note that, for the calculations of the selectivity of the dipolar HETCOR experiment, we considered a Hamiltonian which contains only heteronuclear dipolar coupling terms and which corresponds to selective transfer schemes such as WIM-24 or other isotropic mixing schemes,[5,27] which suppress spin diffusion during heteronuclear polarization transfer. In other words, the homonuclear dipolar couplings between neighboring protons have not been considered. If the dipolar experiment uses simple Hartmann−Hahn cross-polarization, these couplings will lead to a worsening of the selectivity of the dipolar experiment.

None of the spectra that we have so far recorded using the MAS-J-HMQC experiment with τ values less than 2 ms contain cross-peaks with quaternary carbons or with nonbonded protons, which is a good experimental indication that the experiment is as selective as we predict. Note, however, that for longer τ values we expect that the excitation of quaternary carbons by long-range couplings will be comparatively more efficient than that of protonated carbons, due to differences in line widths.

The two experiments also differ in terms of homogeneity of the transfer. The intensity of correlation peaks in the dipolar HETCOR experiment is dependent on the size of the effective heteronuclear couplings. These effective couplings may vary considerably within a molecule. Particularly, some groups may be more mobile than others and, as a result, have smaller effective dipolar couplings. In this case, using a short CP contact time to ensure selectivity will prevent efficient polarization transfer to these groups, and some one-bond correlation peaks will be absent from the 2D spectrum. In contrast, the J_{CH} couplings are much more homogeneous over the molecule. The sensitivity of the MAS-J-HMQC experiment is largely independent of molecular motion or conformation. It is only dependent on the homogeneous line widths of the carbon and proton coherences under FSLG. Finally, we note that there is no intrinsic limitation in terms of spinning frequency to the MAS-J-HMQC experiment. The experiment can be applied at any spinning frequency for which the homonuclear decoupling scheme is efficient (we use FSLG for decoupling, but other schemes are available).

The difference in selectivity between the two experiments can be appreciated in Figure 5, which shows two heteronuclear correlation spectra of a natural abundance sample of L-tyrosine hydrochloride, recorded with the MAS-J-HMQC experiment (a) and with a dipolar HETCOR experiment (transfer through Hartmann−Hahn cross-polarization) (b). The assignment of the 1D CP-MAS spectrum indicated on the top of the figure was obtained from a fully labelled sample of L-tyrosine using the INADEQUATE experiment[28] (data not shown). Note that a dipolar HETCOR experiment on a fully carbon-13 enriched L-tyrosine sample has already been reported.[12] In the MAS-J-HMQC spectrum the CH groups (peaks 2, 5, 6, 7, and 8) yield only one correlation with their attached proton, as expected, whereas there is no correlation for the quaternary carbons (even at lower contour levels). Carbon 3 (a CH_2 group) correlates with two different proton chemical shifts arising from the two diastereotopic protons. In the dipolar HETCOR spectrum (Figure 5b) there are many additional peaks present due to long-range transfer. In particular, the three nonprotonated carbons (peaks 1, 9, and 4) yield correlations with adjacent protons. At lower contour levels, correlations with all types of proton moieties (like the COOH, NH_3^+, or OH) are visible, some of which even correspond to intermolecular correlations. These peaks, which reflect spatial proximities between heteronuclei, can obviously be very useful for structural studies, but they nevertheless greatly complicate the correlation spectrum and render the identification and assignment of the carbon-bonded protons much more difficult. In contrast, assignment is straightforward and unambiguous using the MAS-J-HMQC spectrum for which the

(27) Geen, H.; Titman, J. J.; Spiess, H. *Chem. Phys. Lett.* **1993**, *213*, 145−152.

(28) Lesage, A.; Auger, C.; Caldarelli, S.; Emsley, L. *J. Am. Chem. Soc.* **1997**, *119*, 7867−7868.

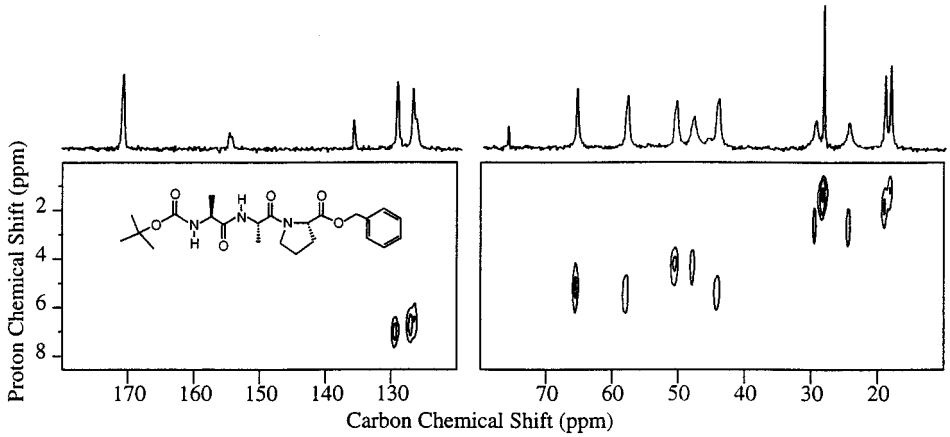

Figure 6. Two-dimensional MAS-J-HMQC spectrum of a natural abundance sample of the tripeptide Boc-Ala-Ala-Pro-O-Bzl. The spinning frequency was 15 kHz and τ was 1.3 ms. A total of 256 t_1 increments with 448 scans each were collected. In the proton dimension we referenced the methyl resonance of the Boc group (see text for details on the assignment of the 2D spectrum) to 1.4 ppm with respect to TMS by analogy with a liquid-state spectrum recorded in $CDCl_3$ at 20 °C.

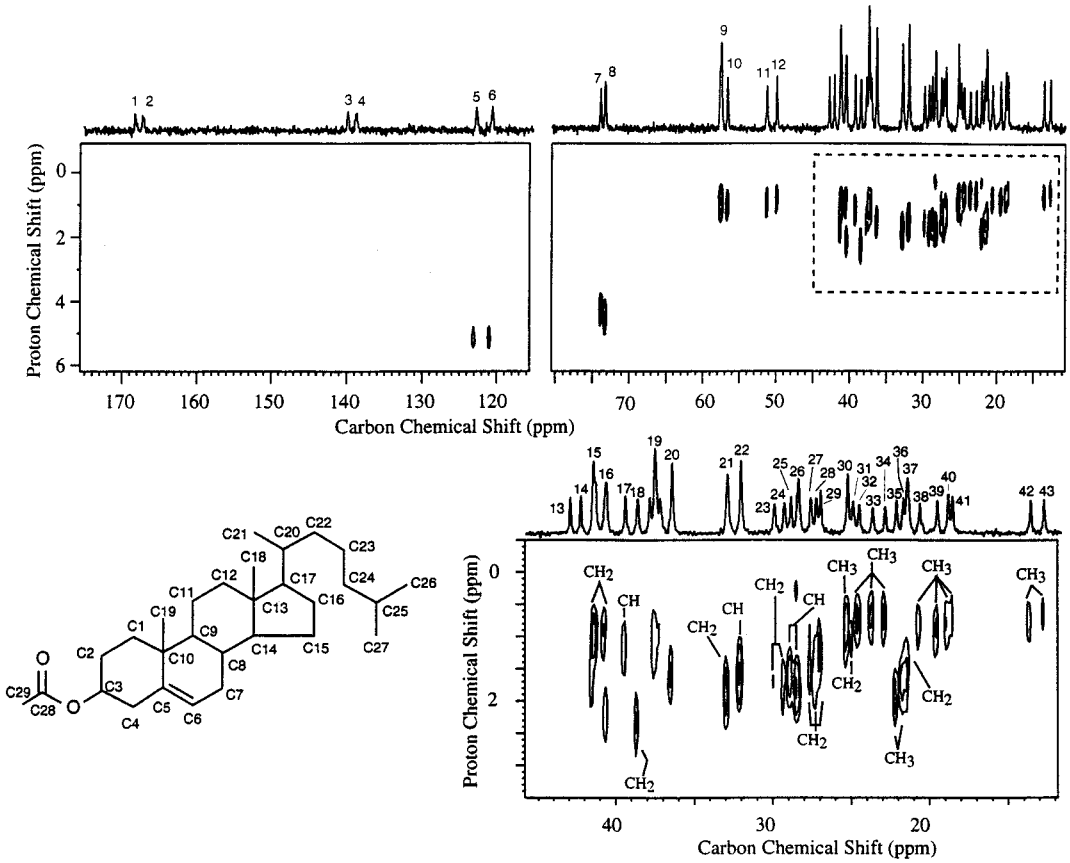

Figure 7. Two-dimensional natural abundance MAS-J-HMQC spectrum of cholesteryl acetate. The spinning frequency was 15 kHz, and τ was 1.3 ms. A total of 140 t_1 increments with 320 scans each were collected. On the expansion of the high-field region of the 2D spectrum, we indicate the identification of the carbon multiplicities as determined by scalar coupling based spectral editing experiments.[14] See Table 2 for details on the proton reference frequency and chemical shifts measured using this spectrum.

effective proton resolution is greatly improved. Of course, the selectivity of the dipolar HETCOR experiment could be improved by using a shorter contact time. However, this would be at the expense of a significant loss in signal intensity, which poses a real problem for natural abundance samples. Under our experimental conditions (cross-polarization contact time of 300 μs for the dipolar HETCOR and a τ delay of 1.3 ms for the MAS-J-HMQC experiment), we found that the sensitivity of the MAS-J-HMQC experiment was approximately half that of the dipolar HETCOR experiment. (Note that, at longer mixing times (τ > 2 ms), weak signals from the quaternary carbons (peaks 1 and 9) appear in the MAS-J-HMQC spectrum. The evolution of the signal intensity of these peaks as a function of τ was found to be compatible with a two-bond J_{CH} coupling transfer.)

In summary, the MAS-J-HMQC experiment provides, both in theory and experiment, intrinsically more selective one-bond correlations than dipolar HETCOR. As such it is a complementary technique to dipolar HETCOR, which remains a powerful method of probing spatial connectivities.

4.3. Application to a Tripeptide. Figure 6 shows the MAS-J-HMQC spectrum recorded for a tripeptide Boc-Ala-Ala-Pro-

O−Bzl. As pointed out above, if the carbon spectrum is assigned, a MAS-J-HMQC experiment leads to the unambiguous assignment of the proton spectrum, thereby allowing the measurement of the proton chemical shifts in solids. For this tripeptide we do not know the assignment of the carbon spectrum. Indeed, whereas several methods have been proposed to characterize MAS spectra of rare nuclei in isotopically enriched compounds, nevertheless the assignment of the carbon spectrum at natural abundance remains a difficult task. In natural abundance samples, correlation with the proton dimension may provide an additional source of information that is useful to characterize the carbon spectrum.

For example, for the tripeptide, we can state without ambiguity that the three carbon resonances at low field as well as the one around 76 ppm, which are not correlated to any proton chemical shift, correspond to quaternary carbons. From carbon chemical shift considerations, the carbon resonance at 76 ppm can be tentatively assigned to the quaternary carbon of the *tert*-butyl group, and that at 136 ppm, to the quaternary carbon of the benzyl group; the remaining two quaternary resonances must therefore correspond to the three amino acid carbonyl groups (170 ppm) and to the carbonyl carbon of the Boc group (155 ppm). The carbon peaks between 126 and 130 ppm yield correlations with the proton dimension at about 7 ppm and are therefore likely to correspond to the protonated carbons of the benzyl group. In the high-field part of the spectrum, 10 correlation peaks can be clearly distinguished, which is exactly the number of expected correlations. The three carbon resonances which correlate with protons around 1.5 ppm (carbon chemical shifts of 18.3, 19, and 28.3 ppm) can be assigned to methyl groups. Tentatively, from carbon chemical shifts, we assume that the peak at 28.3 ppm corresponds to the *tert*-butyl methyl groups, and the other two, to the alanine methyl groups. Of the remaining peaks the two carbons at 24.5 and 29 ppm correlate with protons at around 2.6 ppm and can be therefore tentatively assigned to the proline γ- and β-carbons, respectively. The $O-CH_2$ can be assigned to the peak at 65.8 ppm, which has a proton correlation at 5.2 ppm. The remaining four peaks between 40 and 60 ppm therefore correspond to the proline α- and δ-carbon resonances and to the alanine α-carbons.

Thus, we see how in an unknown spectrum we can go a long way toward assignment without any additional information, simply by analyzing the one-bond carbon−proton correlations which combine carbon and proton chemical shift information.

4.4. Cholesteryl Acetate. In cases where the carbon-13 assignment can be obtained, the amount of detailed information about the proton chemical shifts that can be obtained using these experiments is impressive. We have applied the MAS-J-HMQC experiment to cholesteryl acetate (Figure 7), for which a tentative assignment of the one-dimensional carbon spectrum can be proposed on the basis of carbon-13 spectral editing experiments[14] and comparisons with the fully assigned liquid-state carbon spectrum.[29] As for the tripeptide, proton−carbon chemical shift correlations were used to resolve some of the ambiguities in the assignment. Our assignment is given in Table 2.

This relatively large compound (25 protonated carbons) crystallizes with two molecules per unit cell. Despite the very small proton chemical shift range in the high-field region of the spectrum, the resolution of the 2D map is outstanding. Note that, since the dispersion of the proton spectrum is small, a dipolar HETCOR spectrum on this sample would probably be too complicated to be useful and that the proton spectrum cannot be analyzed by one-dimensional spectroscopy. With the spectrum of Figure 7, we were able to measure for each peak of the one-dimensional carbon spectrum the corresponding proton chemical shift (if present), and the measured values are given in Table 2. The 2D spectrum yields *all of the proton chemical shifts in the molecule*. This is by far the most complex system

Table 2. Proton Chemical Shifts for Solid-State Cholesteryl Acetate Measured from a 2D MAS-J-HMQC Spectrum

peak no.[a]	δ (ppm)[b]	carbon nuclei (tentative assignment)[c]
1	−	C28
2	−	C28
3	−	C5
4	−	C5
5	5.15	C6
6	5.12	C6
7	4.17	C3
8	4.42	C3
9	0.89	*C14*, *C17*
10	0.99	*C14*, *C17*
11	0.90	C9
12	0.80	C9
13	−	C13
14	−	C13
15	0.90, 1.65	*C16*, *C24*
16	2.14, 0.84	*C16*, *C24*
17	1.11	C20
18	2.29	*C4*
19	1.01	C10 and *C22 (C1)*
20	1.54	C10 and *C1 (C22)*
21	1.78	C7
22	1.53	C8
23	1.63	*C2* (*C15*, *C12*)
24	1.72	*C2* (*C15*, *C12*)
25	1.56	C25
26	1.75	C25
27	1.49	*C15*, *C12* (*C2*)
28	1.59	*C15*, *C12* (*C2*)
29	1.19	*C15*, *C12* (*C2*)
30	0.77	*C27* (*C26*)
31	0.97	*C23*
32	0.67	*C27* (*C26*)
33	0.65	*C26* (*C27*)
34	0.66	*C26* (*C27*)
35	1.85	C29
36	1.65	C29
37	1.49	C11
38	0.78	*C19* (*C21*)
39	0.86	*C19* (*C21*)
40	0.78	*C21* (*C19*)
41	0.64	*C21* (*C19*)
42	0.73	C18
43	0.65	C18

[a] Peak number in the one-dimensional carbon spectrum of cholesteryl acetate as indicated in Figure 7. [b] In the proton dimension, we referenced the proton signal which correlates to carbon peak 43 at 0.65 ppm with respect to TMS by analogy to a liquid-state spectrum recorded in $CDCl_3$ at 20 °C. This peak corresponds to the methyl group 18 of one of the two cholesteryl acetate molecules in the unit cell. Errors on the reported chemical shifts are estimated to be around ± 0.05 ppm. [c] The proposed assignment of the carbon one-dimensional spectrum was done by combining previous spectral editing experiments[14] with the knowledge of the proton and carbon[29] spectra in the liquid state. We report the unambiguous assignments in plain text and those for which there are uncertainties in italic. For the uncertain peaks we have put the most probable assignment first, with potential alternatives in parentheses.

(29) Reich, H. J.; Jautelat, M.; Messe, M. T.; Weigert, F. J.; Roberts, J. D. *J. Am. Chem. Soc.* **1969**, *91*, 7445.
(30) Bodenhausen, G.; Kogler, H.; Ernst, R. R. *J. Magn. Reson.* **1984**, *58*, 370.
(31) Sorensen, O. W.; Eich, G. W.; Levitt, M. H.; Bodenhausen, G.; Ernst, R. R. *Prog. Nucl. Magn. Reson. Spectrosc.* **1983**, *16*, 163−192.
(32) Hediger, S. Ph.D. Thesis, ETH Zurich, 1997.

for which proton chemical shifts in the solid state have ever been reported.

5. Conclusions

In conclusion, we have shown that scalar J_{CH} couplings can be used to create heteronuclear multiple-quantum coherence in ordinary organic solids. A new two-dimensional carbon−proton correlation experiment has been proposed, yielding cross-peaks between pairs of *bonded* heteronuclei in natural abundance compounds. Unlike previously proposed heteronuclear correlation experiments, based on dipolar couplings, the technique is highly selective and therefore allows the unambiguous identification of proton chemical shifts in powdered solids. We have used the technique on model samples, as well as on a tripeptide and on cholesteryl acetate. The example of cholesteryl acetate is the first example of the proton assignment of such a complex system in the solid-state and demonstrates the enormous potential of these experiments. In addition, correlations with the proton dimension can be very useful to characterize the carbon spectrum in natural abundance sample. The technique, which is complementary to the dipolar HETCOR experiment, should be applicable to a wide variety of crystalline and amorphous compounds and is expected to become widespread for proton spectral characterization in solids. This is the first example of this type of spectroscopy in solids, and one can immediately imagine many derivative experiments (as has been the case in liquids). By way of example, a proton−nitrogen-15 MAS-J-HMQC experiment should also be practicable and useful to characterize the amide protons in natural abundance or labeled polypeptide chains.

Acknowledgment. The authors thank Dr. Laure Guy and Dr. Joëlle Vidal for the sample of the Boc-Ala-Ala-Pro-O-Bzl tripeptide.

JA983048+